JACS
JOURNAL OF THE AMERICAN CHEMICAL SOCIETY

Article

pubs.acs.org/JACS

Photophysics of Threaded sp-Carbon Chains: The Polyyne is a Sink for Singlet and Triplet Excitation

Levon D. Movsisyan,[†] Martin D. Peeks,[†] Gregory M. Greetham,[‡] Michael Towrie,[‡] Amber L. Thompson,[†] Anthony W. Parker,*[,‡] and Harry L. Anderson*[,†]

[†]Department of Chemistry, University of Oxford, Chemistry Research Laboratory, Mansfield Road, Oxford OX1 3TA, United Kingdom

[‡]Central Laser Facility, Research Complex at Harwell, Science and Technology Facilities Council, Harwell Oxford, Didcot OX11 0QX, United Kingdom

Supporting Information

ABSTRACT: We have used single-crystal X-ray diffraction and time-resolved UV−NIR−IR absorption spectroscopy to gain insights into the structures and excited-state dynamics of a rotaxane consisting of a hexayne chain threaded through a phenanthroline macrocycle and a family of related compounds, including the rhenium(I) chlorocarbonyl complex of this rotaxane. The hexayne unit in the rhenium-rotaxane is severely nonlinear; it is bent into an arc with an angle of 155.6(1)° between the terminal C1 and C12 atoms and the centroid of the central C−C bond, with the most acute distortion at the point where the polyyne chain pushes against the $Re(CO)_3Cl$ unit. There are strong through-space excited-state interactions between the components of the rotaxanes. In the metal-free rotaxane, there is rapid singlet excitation energy transfer (EET) from the macrocycle to the hexayne (τ = 3.0 ps), whereas in the rhenium-rotaxane there is triplet EET, from the macrocycle complex ^{3}MLCT state to the hexayne (τ = 1.5 ns). This study revealed detailed information on the short-lived higher excited state of the hexayne (lifetime ∼1 ps) and on structural reorganization and cooling of hot polyyne chains, following internal conversion (over ∼5 ps). Comparison of the observed IR bands of the excited states of the hexayne with results from time-dependent density functional calculations (TD DFT) shows that these excited states have high cumulenic character (low bond length alternation) around the central region of the chain. These findings shed light on the complex interactions between the components of this supramolecular rotaxane and are important for the development of materials for the emerging molecular and nanoscale electronics.

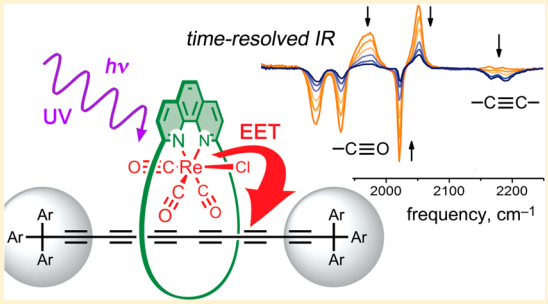

INTRODUCTION

Polyynes, and materials based on chains of linear sp carbon atoms, have long been a focus of research, as models for carbyne, the elusive 1D allotrope of carbon.[1] This field has been stimulated by the extraordinary mechanical,[2] charge-transport,[3−6] and nonlinear optical[7] properties of these materials and by the use of polyynes as precursors to other carbon-rich nanostructures.[8] Recently, Chalifoux and Tykwinski developed efficient methods for preparing end-capped polyynes with up to 22 C≡C units[9] (the longest polyyne yet isolated, corresponding to a rod of carbyne of length 5.6 nm). The stabilities of polyynes generally decrease as the acetylenic chains become longer, suggesting that supramolecular encapsulation may be a valuable strategy for controlling reactivity.[10−15] In this context, we,[16] and others,[17] reported the synthesis of polyyne rotaxanes, such as **H⊂M** in which a phenanthroline-based macrocycle **M**[18] is threaded around a hexayne chain **H** (Chart 1). These rotaxanes provide an opportunity to control the environment of the polyyne chain, for example, we showed that rhenium(I) can be complexed to the threaded macrocycle to give **H⊂M(Re)**, in which a $Re(CO)_3Cl$ unit is held in contact with the hexayne core. Most phenanthroline-$Re(CO)_3Cl$ complexes exhibit bright luminescence,[19−22] but during our initial study we found that the luminescence of **M(Re)** is totally quenched in **H⊂M(Re)**. This result was surprising because the HOMO−LUMO gap of the hexayne (absorption λ_{max} 315 nm) appears to be too large to accept excitation from the $Re(CO)_3Cl$ unit (emission λ_{max} 605 nm), while the electron affinity of the polyyne is insufficient for it to quench the rhenium luminescence by photoinduced electron transfer.[23,24]

Here we present a detailed investigation of the five compounds shown in Chart 1, using two ultrafast pump−probe techniques: UV−NIR transient absorption (TA) and time-resolved infrared (TRIR) spectroscopy, both with pumping at UV wavelengths. The results provide many insights into the photophysics of polyyne chains and reveal that the luminescence quenching in **H⊂M(Re)** originates from rapid triplet energy migration from the lowest metal-to-ligand charge transfer (^{3}MLCT) excited state of **M(Re)** to the threaded hexayne (time constant: τ = 1.5 ns).

Received: September 2, 2014
Published: December 4, 2014

   dx.doi.org/10.1021/ja510663z | J. Am. Chem. Soc. 2014, 136, 17996−18008

Chart 1. Structures of the Compounds Investigated in this Study

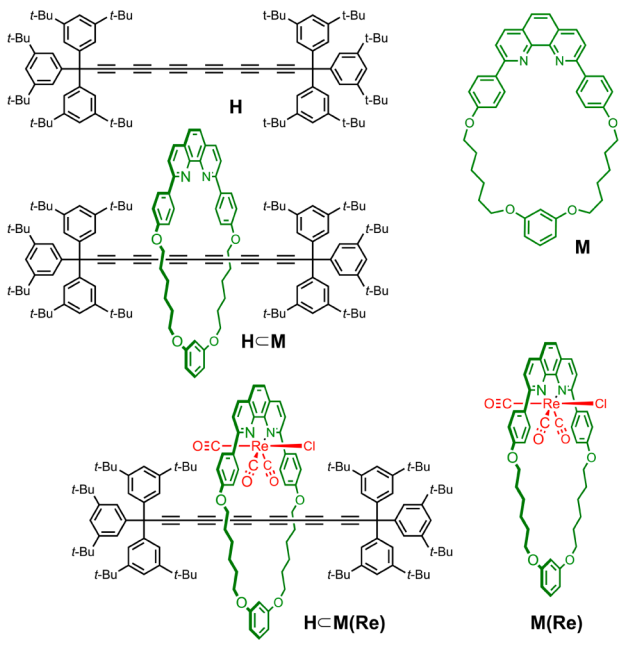

TRIR is an excellent technique for examining the kinetics of transient species, with a time-resolution of <200 fs.[25] When investigating the photophysics of polyynes, strong signals are observed for the C≡C triple-bond stretch (2100−2200 cm^{-1}), providing information on ground-state depletion and recovery (through the negative ΔA "bleach" signal) and probing the evolution of singlet and triplet excited states, which can be distinguished by their different C≡C stretch frequencies (reflecting their different extents of bond length alternation). Despite these attractive features, there have been no previous ultrafast TRIR studies of polyynes,[26] which is surprising because, despite extensive investigation, the excited states of polyynes remain poorly understood. Theoretical and experimental studies agree that the first singlet excited states (S_1) are generally "dark states", which means that S_0−S_1 transitions are dipole forbidden.[27−36] Consequently, the absorption spectra are dominated by transitions to higher singlet excited states ($S_0 \rightarrow S_n$), while the $S_0 \rightarrow S_1$ absorption band is weak or unobservable. Internal conversion (IC, $S_n \rightarrow S_1$) is very rapid, but fluorescence from S_1 is normally too slow to compete with intersystem crossing (ISC, $S_1 \rightarrow T_1$) and nonradiative decay (IC, $S_1 \rightarrow S_0$). Unsubstituted polyynes, H−(C≡C)$_n$−H, exhibit an intense allowed absorption band to a high-energy singlet state ($^1\Sigma^+_g \rightarrow {}^1\Sigma^+_u$) as well as weak absorption bands at longer wavelengths, which are about 1000-times less intense and involve low-lying singlet states ($^1\Sigma^+_g \rightarrow {}^1\Sigma^-_u$ and $^1\Sigma^+_g \rightarrow {}^1\Delta_u$).[27−30] Other polyynes, R−(C≡C)$_n$−R, show similar behavior,[31−36] although their electronic structures can be complicated by involvement of the end groups (particularly if R = aryl), and it can be difficult to identify the dark states. Knowledge of the energy of the dark S_1 state is essential for estimating the optical HOMO−LUMO gap and for understanding charge transport.[3−6] Computational studies have shown that the excited states of polyynes generally have reduced bond length alternation, i.e., the C≡C triple bonds become longer and the C−C single bonds become shorter.[35,37,38] This prediction is supported by analysis of vibrational structure in electronic transitions[28] and by time-resolved resonance Raman studies on the T_1 state of diphenyl butadiyne (Ph−C≡C−C≡C−Ph),[39] and an intriguing metastable photoexcited polyyne has been identified at low temperatures which appears to have a cumulenic structure (=C=C= rather than −C≡C−).[40] Here we present the first TRIR study of an extended polyyne. We show that optical excitation generates a short-lived higher singlet state (S_n) with a lifetime of 0.9 ps in the free hexayne **H** and 1.8 ps in the rotaxane **H⊂M**. TRIR also enables the S_1 and T_1 states of the polyyne to be directly observed; comparison of the C≡C stretch frequencies (S_0: 2191, 2165 cm^{-1}; S_1: 2077, 1737 cm^{-1}; T_1: 2047, 1610 cm^{-1}) with results from DFT calculations provides clear evidence for an increase in cumulenic character in the excited states. We also observe ultrafast singlet excitation energy transfer (EET) in **H⊂M**, from the singlet excited state of the macrocycle to the dark S_1 state of the polyyne (EET, τ = 3.0 ps). The TRIR spectra show that this energy-transfer process directly populates the vibrationally equilibrated S_1 state of the hexayne, whereas $S_n \rightarrow S_1$ internal conversion creates a hot vibrational state, which cools over about 5 ps.

To gain more insights into this family of compounds, we have also compared the X-ray crystal structures of **H**, **H⊂M**, **H⊂M(Re)**, and **M(Re)**. The structure of the **H⊂M(Re)** rotaxane complex shows that the Re(CO)$_3$Cl unit is pushed close to the C$_{12}$ chain, with O···C distances of less than the sum of the van der Waals radii, with the polyyne bending round the metal center. The interactions between the Re(CO)$_3$Cl center and the hexayne chain appear to be weak in the ground state, while the excited-state TRIR spectra revealed mutual electronic perturbation of both components.

EXPERIMENTAL SECTION

Materials. The unthreaded hexayne dumbbell **H**,[9] rotaxane **H⊂M**, Re(CO)$_3$Cl·rotaxane **H⊂M(Re)**, and Re(CO)$_3$Cl·macrocycle **M(Re)** complexes[16] and macrocycle **M**[18] were prepared as described previously. Spectroscopic measurements were performed in air-saturated or deoxygenated dichloromethane solutions of spectroscopic quality (Aldrich). Deoxygenation was achieved by three freeze−pump−thaw cycles, and sample preparation was carried out in glovebox under nitrogen atmosphere.

Crystallography. The crystal structures of hexayne dumbbell **H** and rotaxane **H⊂M** were reported previously.[9,16] Crystals of Re(CO)$_3$Cl·macrocycle **M(Re)** were grown by slow evaporation of a solution in toluene at 4 °C; single crystal X-ray diffraction data were collected at 150 K using an Oxford Diffraction (Agilent) SuperNova A diffractometer. Crystals of the Re(CO)$_3$Cl·rotaxane complex **H⊂M-(Re)** were grown from dichloromethane solutions by slow diffusion of methanol vapor at room temperature; single crystal X-ray diffraction data were collected at 100 K using synchrotron radiation at the Diamond Light Source, beamline I19.[41] In both cases, data were reduced using CrysAlisPro. **M(Re)** was found to crystallize in *P*-1 with one molecule of **M(Re)** and two molecules of toluene in the asymmetric unit, while **H⊂M(Re)** crystallized in $P2_1/n$ with one molecule of **H⊂M(Re)** in the asymmetric unit. The structures were solved using charge flipping[42] with SuperFlip[43] and refined using least-squares within CRYSTALS.[44] The difference map for **H⊂M(Re)** indicated the presence of diffuse electron density believed to be disordered solvent. SQUEEZE[45] was used leaving a void from which the electron density was removed. Full refinement details are given in the SI (CIF). Crystallographic data (excluding structure factors) have been deposited with the Cambridge Crystallographic Data Centre (CCDC 1036072−1036073), and copies of these data can be obtained free of charge via www.ccdc.cam.ac.uk/data_request/cif.

Time-Resolved Spectroscopy. The ULTRA instrument at the STFC Rutherford Appleton Laboratory was used and is described in

dx.doi.org/10.1021/ja510663z | J. Am. Chem. Soc. 2014, 136, 17996−18008

detail elsewhere.[46] Briefly, an amplified titanium sapphire laser (Thales Optronique) produces ~50 fs pulses at a 10 kHz repetition rate. The laser fundamental output (800 nm) is split into two parts. The first generates UV pump pulses through an optical parametric amplifier (TOPAS OPA) at 310 or 350 nm. The second part of the fundamental is used to generate probe pulses: ~400 cm^{-1} broad mid-IR probe pulses through a second OPA for TRIR experiments or a white light continuum (330−680 nm) through focusing of the fundamental into a 2 mm CaF_2 plate for TA experiments. Typical pump and probe beam diameters in the sample were 130 and 80 μm, respectively, the lower diameter probe being used to ensure only activated sample is interrogated. UV pump pulse energy was kept around 0.1 μJ. All experiments were carried out with the pump and probe set at the magic angle (54.7°). The probe pulses were split in two, one part subsequently focused into the sample overlapping with the pump beam and the other for use as a reference of laser spectral and intensity variations. The probe and reference pulses were dispersed onto array detectors to measure the spectrum of each laser shot (using 128-element HgCdTe detectors for TRIR experiments and 512-pixel silicon single-diode arrays for TA experiments). By modulating the pump pulses at 5 kHz (the probe measured at 10 kHz) normalized pump on−pump off difference spectra can be collected in real time. The TRIR and TA spectra (see below) are presented as normalized difference spectra (each spectrum averaged over a few seconds), thus, positive bands correspond to photogenerated TA, while negative bands indicate ground-state bleaching.

The pump−probe time delay was controlled by an optical delay line for femtosecond to nanosecond measurements, while the nanosecond to microsecond measurements were recorded using the same spectrometers but replacing the femtosecond pump laser with a 1 ns duration 5 kHz (for pump on−pump off measurements as above) laser operating at 266 nm.

The sample absorbance was 0.2−0.3 at the pump wavelength (266, 310 or 350 nm) in a 0.1 mm path length flow cell with 2 mm CaF_2 windows. The cell was raster-scanned to avoid sample decomposition on window surfaces. Sample integrity was checked by IR and UV−vis spectra measured before and after each experiment. All spectral fitting procedures and kinetic analysis were performed using OriginPro 8.5.1 software. TA spectra were corrected for group velocity dispersion over the wide spectral range.

Computational Methods. (TD)DFT calculations were performed using TURBOMOLE version 6.1.[47] The hexayne **H** was modeled as a methyl-capped hexayne, Me−C_{12}−Me. The applicability of this model was assessed by comparison to bent structures and a *tert*-butyl capped model (cf. ref 40). The B3LYP functional was used in conjunction with the Dunning cc-pVTZ basis set.[48] This level of theory has been shown to reproduce vibronic structures of polyyne absorption bands.[36] Similar results were obtained with B3LYP/6-31G**, PBE0/cc-pVTZ, and PBE0/6-31G** (see SI).[49] The ground state (S_0) was optimized in D_3 symmetry. The first singlet excited state (S_1) was optimized in D_3 symmetry using TD-DFT (B3LYP). The first triplet excited state (T_1) was treated with UB3LYP, in C_2 symmetry. Calculations on S_0 and T_1 made use of the RI-J approximation.[50] Vibrational frequencies were calculated from analytical force constants for S_0 and T_1 and from numerical force constants (TD-DFT) for S_1. The converged structures were confirmed to be minima by the absence of imaginary frequencies. A simple linear scaling factor (0.96) is applied to calculated vibrational frequencies presented in the main text (unscaled frequencies are tabulated in the SI).

RESULTS AND DISCUSSION

Crystallographic Analysis. The structures of the hexayne dumbbell **H**,[9] rotaxane **H⊂M**,[16] rhenium rotaxane **H⊂M(Re)**, and rhenium-macrocycle complex **M(Re)** are compared in Figure 1. The two rotaxanes, **H⊂M** and **H⊂M(Re)**, show similar bond length alternation within experimental error: 0.143 ± 0.008 Å in **H⊂M** and 0.155 ± 0.010 Å in **H⊂M(Re)**, compared with 0.158 ± 0.008 Å for **H**.[9,16] The closest distance between carbonyl group oxygen and polyyne chain carbon in

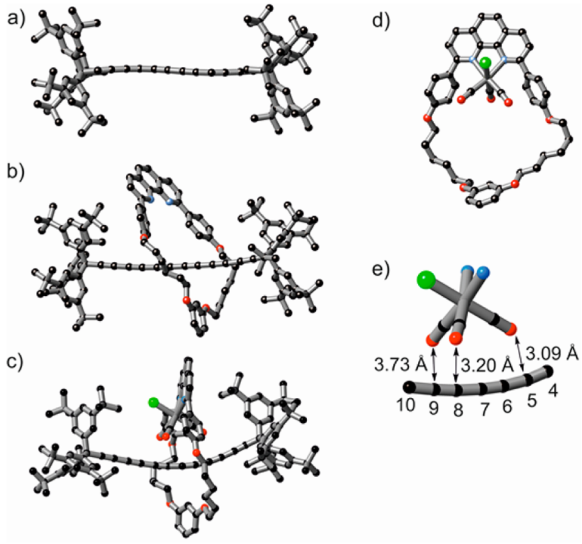

Figure 1. Solid-state structures of (a) hexayne **H**, (b) rotaxane **H⊂M**, (c) $Re(CO)_3Cl$·rotaxane **H⊂M(Re)**, and (d) $Re(CO)_3Cl$·macrocycle **M(Re)**. Short CO···C contacts in **H⊂M(Re)** are shown (e). H atoms and solvent molecules are omitted for clarity.

H⊂M(Re) is 3.085(5) Å (CO−C(5)), which is less than the sum of the van der Waals radii (3.35 Å);[51] the three shortest CO···C≡C contacts are shown in Figure 1e.

The hexayne chain in **H⊂M(Re)** is severely bent, with a single-arc conformation, unlike the double-arc of **H**.[9,52] The angle between the two terminal C1 and C12 atoms and the centroid of the middle C6−C7 bond of **H⊂M(Re)** is 155.6(1)° (compared with 171.8(1)° in **H⊂M** and 180° in **H**); the average value for this parameter for the 22 hexaynes in the Cambridge Structural Database[53] is 175.3° (s.d. 7.1°),[7a,9,12,13,16,54,55] and only one other hexayne has been reported with a comparable angle (155.3(2)°).[55] The angles between the three carbonyl groups lie in the range 85.20(17)−92.55(17)° (with an average of 88.7°) in **H⊂M(Re)** and 85.47(16)−90.53(16)° (with an average of 87.9°) in **M(Re)**, and the local C_s symmetry of the rhenium center is preserved in both $Re(CO)_3Cl$ complexes (Figure 1).

Ground-State UV Absorption and IR Spectra. The UV absorption spectrum of hexayne **H** in dichloromethane (Figure 2a) shows an intense band at 275−325 nm, with a well-defined progression of ~2060 cm^{-1}, corresponding to the C≡C vibrational mode of the S_n state.[9,27−36,56] The vibrational progression matches well with the ground-state C≡C stretch frequency (2165−2191 cm^{-1}) seen in the IR spectrum (Figure 2b). Hexayne **H** also displays a weak absorption band at 350−450 nm, dominated by a vibrational progression of 2040−2169 cm^{-1} (inset in Figure 2a). We assign this band to the forbidden $S_0 \rightarrow S_1$ transition, as reported in the absorption spectra of many other long polyynes,[27−36] although we cannot exclude the possibility that it is a transition to another low-lying singlet excited state, other than S_1. This $S_0 \rightarrow S_1$ transition at 350−450 nm is about 500 times weaker than the $S_0 \rightarrow S_n$ absorption at 275−325 nm. For the **H⊂M** rotaxane, the third vibrational band of the $S_0 \rightarrow S_1$ transition is obscured by the intense absorption of macrocycle at ~390 nm, but the first two bands are clearly visible and do not change their position, while in the **H⊂M(Re)** rotaxane, all the $S_0 \rightarrow S_1$ transitions are hidden by the intense **M(Re)** absorption.

dx.doi.org/10.1021/ja510663z | J. Am. Chem. Soc. 2014, 136, 17996−18008

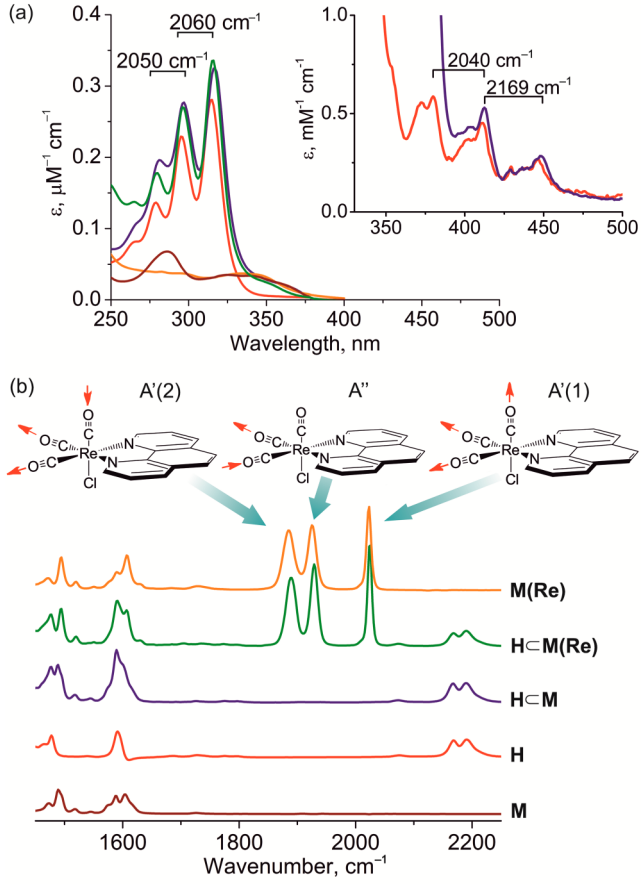

Figure 2. (a) UV−vis absorption and (b) IR spectra of the hexayne **H** (red), the rotaxane **H⊂M** (blue), **H⊂M(Re)** (green), **M(Re)** (orange), and **M** (brown), all recorded in CH_2Cl_2. Concentrations of the compounds for IR measurements are 1.5 mM; path length 0.5 mm. (a) Insert depicts the weak $S_0 \rightarrow S_1$ absorption. (b) The top picture depicts the three stretching modes of carbonyl groups.[61] The same color code is used for spectra in (a) and (b).

The absorption spectrum of the macrocycle **M** (Figure 2a) consists of a broad, lower energy $\pi-\pi^*$ band, extending to 390 nm, and a $n-\pi^*$ band at around 275 nm.[57] The absorption spectrum of the rotaxane **H⊂M** is essentially the sum of its two components, thread and dumbbell, with a slight (~4 nm) bathochromic shift of the hexayne peaks (Figure 2a); the presence of the threaded macrocycle slightly changes the environment of the polyyne chain. Similar results were obtained for $Re(CO)_3Cl$ complexes. The **M(Re)** absorption spectrum consists of two transitions: a low-energy MLCT, extending to about 490 nm, and a higher energy intraligand (IL) $\pi-\pi^*$ transition.[58] The spectrum of the **H⊂M(Re)** is the sum of its components with a slight (~2 nm) red-shift in the hexayne peaks (Figure 2a).

IR spectra were measured in dichloromethane (Figure 2b). The hexayne **H** has a broad collective band with two overlapping peaks at 2165 and 2191 cm^{-1}, which are characteristic of long polyyne chains.[40,59,60] The assignment of these bands is discussed below (see section on calculated IR spectra). These C≡C bands are unshifted in the rotaxanes **H⊂M** and **H⊂M(Re)**, indicating that threading does not perturb the ground-state vibrational structure of hexayne. The three carbonyl groups of the $Re(CO)_3Cl$ moiety give rise to three sharp, intense bands at 1894 (A′(2)), 1932 (A″), and 2025 (A′(1)) cm^{-1} for **H⊂M(Re)** and 1885 (A″), 1924 (A′(2)), and 2022 (A′(1)) cm^{-1} for **M(Re)**, which are characteristic of *fac*-rhenium tricarbonyl polypyridyl complexes.[61] The positions of the IR bands indicate the C_s (or pseudo C_3) symmetry of the Re center: two normal ν(CO) modes are symmetric (A′(1) and A′(2)) involving all three CO ligands, while one mode (A″) is antisymmetric involving only in the plane stretching of two CO groups (Figure 2b). On threading, the A″ and A′(2) bands of $Re(CO)_3Cl$·macrocycle **M(Re)** shift to higher wavenumber, by 8 and 9 cm^{-1}, respectively. The relative intensities of all CO bands are similar in both $Re(CO)_3Cl$ complexes.

Time-Resolved Spectroscopy. We carried out a systematic study of the dynamic processes in the excited states of this family of compounds, using TRIR and TA spectroscopy. Initially, we examined the excited-state behavior of the hexayne **H** and the macrocycle **M** separately, and then we moved to the topologically more complex rotaxane **H⊂M**, rhenium tricarbonyl complex of macrocycle **M(Re)**, and rhenium tricarbonyl rotaxane complex **H⊂M(Re)**. Two regions of the TRIR spectra are particularly informative: the high-frequency region at 1900−2300 cm^{-1} and the "fingerprint" region at 1400−1900 cm^{-1}. The kinetic data for **H**, **H⊂M** and **H⊂M(Re)** are summarized in Tables 1−4.

Table 1. Excited-State Bands, Transitions, and Lifetimes for Hexayne H in CH_2Cl_2 Excited at 310 nm

TRIR band (cm^{-1})	lifetime (τ)	assignment
2077	0.44 ± 0.02 ns	$S_1 \rightarrow T_1$ decay
2047	0.48 ± 0.05 ns	$S_1 \rightarrow T_1$ growth
1737	0.40 ± 0.04 ns	$S_1 \rightarrow T_1$ decay
1610	0.38 ± 0.02 ns	$S_1 \rightarrow T_1$ growth
1610[a]	16.0 ± 3.6 μs	$T_1 \rightarrow S_0$ decay
TA band (nm)	lifetime (τ)	assignment
421	0.44 ± 0.02 ns	$S_1 \rightarrow T_1$ decay
343	0.45 ± 0.01 ns	$S_1 \rightarrow T_1$ growth
421	0.93 ± 0.08 ps	$S_n \rightarrow S_1$ growth
1085	0.82 ± 0.13 ps	$S_n \rightarrow S_1$ decay

[a]Excited at 266 nm and measured in O_2-free CH_2Cl_2.

Hexayne H. Excitation of hexayne **H** at 310 nm results in an immediate bleach of the ground-state C≡C stretch at 2165−2191 cm^{-1} (within the time-resolution of our instrument, <200 fs), and a new absorption band appears at 2063 cm^{-1} (Figure 3a). This band, which corresponds to the C≡C stretch in a singlet excited state, shifts to 2077 cm^{-1} (τ = 0.8 ± 0.2 ps, Figures 3a and S3a) in parallel with a ~15% band narrowing (measured at the half-maximum). These two spectral changes are indicative of rapid excited-state vibrational energy redistribution, convolved with solvent reorganization around the nascent excited state,[62] and fast $S_n \rightarrow S_1$ internal conversion, as discussed below. Previously, the formation of a vibrationally hot polyyne upon vertical excitation was postulated from the broadness of the TA spectra at short time delays.[32] To our knowledge, this is the first time that the vibrational relaxation of a "hot" excited long polyyne has been characterized via vibrational spectroscopy.

The S_1 band at 2077 cm^{-1} decays to a new band at 2047 cm^{-1} (Figure 3b) which we assign to the T_1 triplet excited-state C≡C stretch (based on the kinetics and on the match with calculated vibrational frequencies; see below); the rates of this decay (τ_1 = 0.44 ± 0.02 ns) and of the growth of the band at

dx.doi.org/10.1021/ja510663z | J. Am. Chem. Soc. 2014, 136, 17996−18008

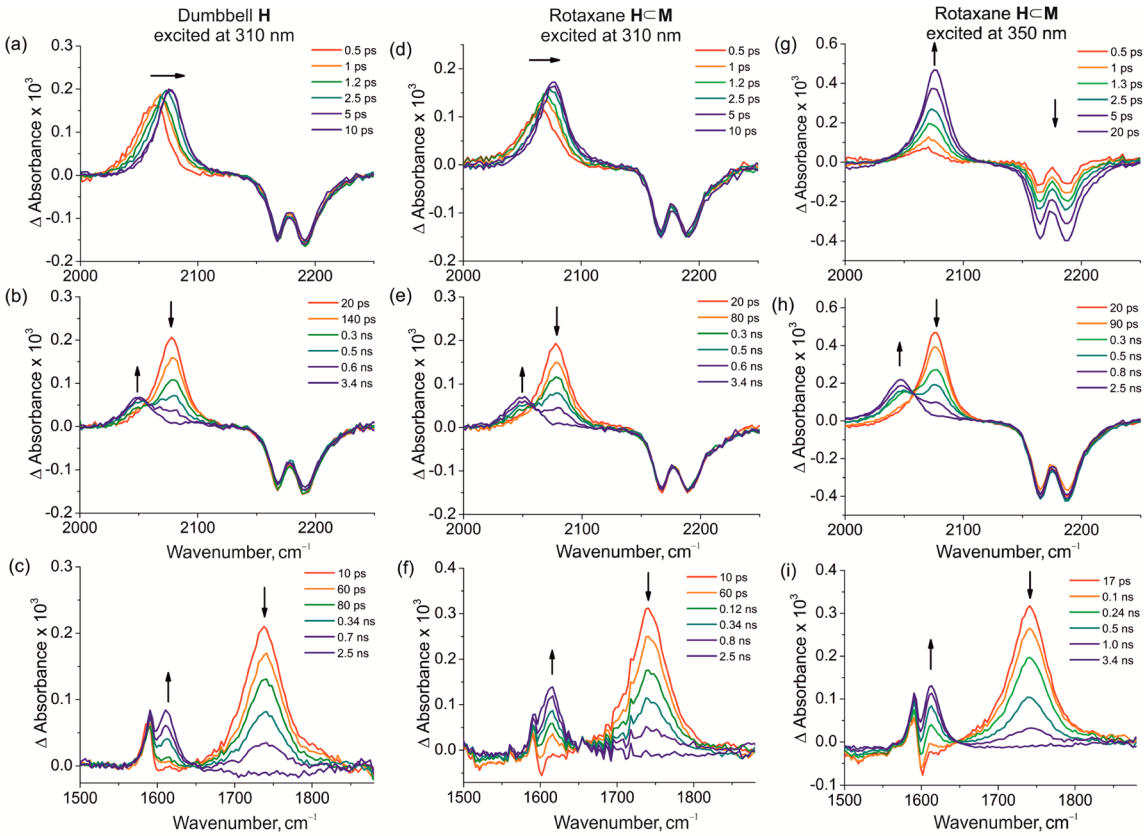

Figure 3. TRIR spectra and excited-state kinetics of hexayne dumbbell **H** excited at 310 nm (a–c), rotaxane **H⊂M** excited at 310 nm (d–f) and 350 nm (g–i). Laser energy: 80–100 nJ, solvent: CH_2Cl_2.

2047 cm^{-1} (τ_2 = 0.48 ± 0.05 ns, Figure S1c) give the rate of ISC, as summarized in Table 1. The intensity of the C≡C ground-state bleach band at 2175–2195 cm^{-1} does not change during ISC, indicating that the triplet yield is near unity.

Spectacular changes are also observed in the fingerprint region (Figure 3c), and these are useful for confirming the species assignments and associated kinetics. Immediately after excitation, a band appears at ∼1740 cm^{-1}, which decays gradually, giving a new band at 1610 cm^{-1}. These two bands display similar kinetics (1740 cm^{-1} decay time: τ_1 = 0.40 ± 0.04 ns; 1610 cm^{-1} rise time: τ_2 = 0.38 ± 0.02 ns, Figure S1e) to the bands at 2040–2080 cm^{-1} and are attributed to the same excited species, $S_1 \rightarrow T_1$. TD DFT calculations provide assignments for these low-energy excited-state IR bands, as discussed below (see section on calculated IR spectra). The lifetime of the T_1 state of **H** in deoxygenated dichloromethane is 16.0 ± 3.6 μs (estimated from the 1610 cm^{-1} band; excitation with a 1 ns pulse at 266 nm; Figure S2).

At early times, the fingerprint band of the singlet excited state at 1741 cm^{-1} shifts to 1737 cm^{-1}, while decreasing in intensity, over 3 ps (Figure S3b). The direction of this spectral shift is opposite to that expected for intramolecular relaxation and solvation processes, and we tentatively assign it to the formation of S_1 by internal conversion from S_n, populated by a symmetry-allowed S_0–S_n transition. TA spectra show a similar fast process: Excitation at 310 nm generates a band at 421 nm, which grows with a rise time of τ_1 = 0.93 ± 0.08 ps (Figure 4). This rise is too slow for direct vertical excitation (in TRIR spectra the bleach of ground-state C≡C stretching appears within the 200 fs instrument time-resolution). Thus, the most reasonable explanation is the formation of the S_1 state via the

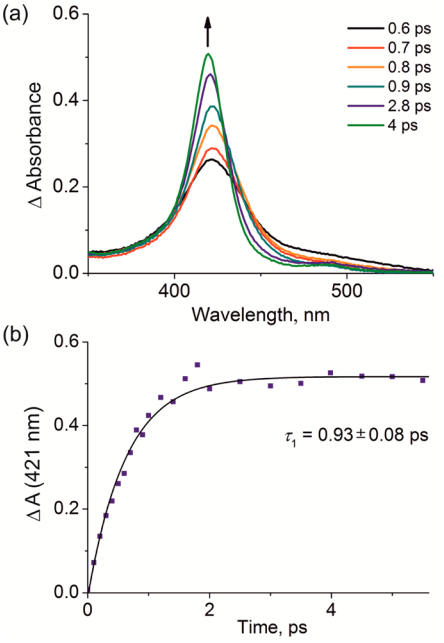

Figure 4. Growth of the S_1 state of hexayne **H** following excitation at 310 nm in CH_2Cl_2: (a) TA spectra and (b) signal at 421 nm (τ_1 = 0.93 ± 0.08 ps).

symmetry-allowed $S_0 \rightarrow S_n$ transition. At longer times, TA confirms that the S_1 state undergoes intersystem crossing, resulting in a band at 343 nm, corresponding to the T_1 state (Figure 5a). The kinetics of T_1 band growth at 343 nm (τ_2 =

dx.doi.org/10.1021/ja510663z | J. Am. Chem. Soc. 2014, 136, 17996–18008

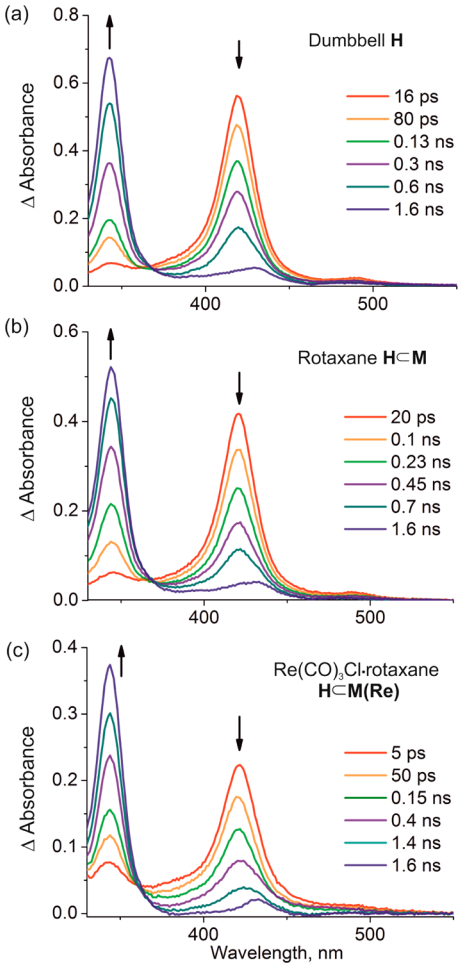

Figure 5. TA spectra of (a) hexayne **H**, (b) rotaxane **H⊂M**, and (c) $Re(CO)_3Cl$·rotaxane **H⊂M(Re)** excited at 310 nm. Laser energy: 100–200 nJ; solvent: CH_2Cl_2.

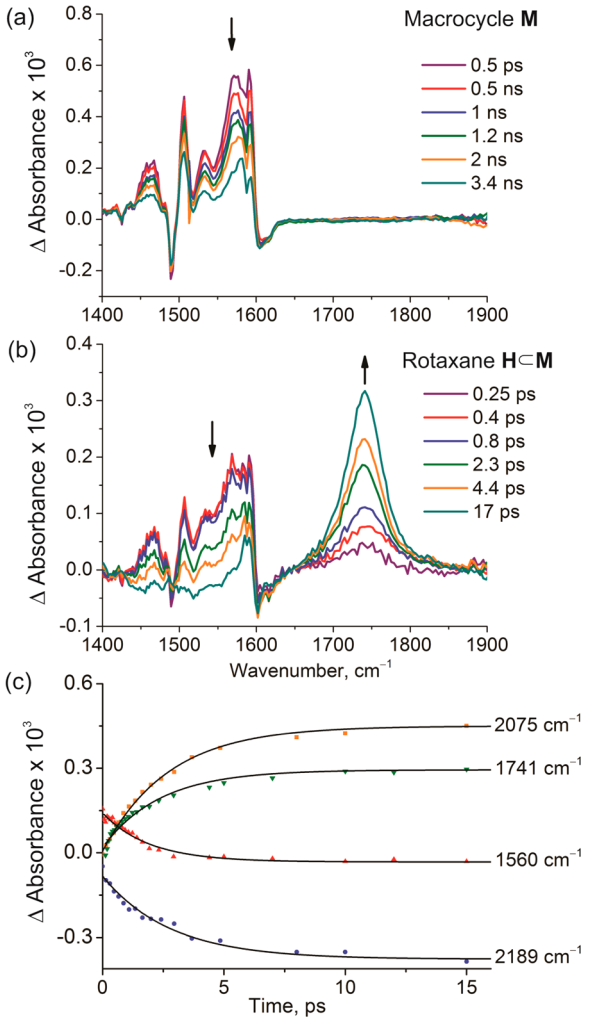

Figure 6. TRIR spectra of (a) macrocycle **M** and (b) rotaxane **H⊂M** excited at 350 nm. (c) Kinetics of the singlet EET from **M** to the dumbbell estimated from the different spectral regions and bands, excited at 350 nm. Laser energy: 45 nJ; solvent: CH_2Cl_2.

0.45 ± 0.09 ns) and S_1 decay (τ_1 = 0.44 ± 0.02 ns; Figure S4) are similar to those extracted from TRIR spectra.

Examination of the NIR TA showed a short-lived broad band at 1185 nm which appears immediately following the excitation pulse (Figure S5). The decay time of this band (τ_1 = 0.82 ± 0.13 ps; Figure S5b) matches the growth of the S_1 state in the visible region of TA spectrum (τ_1 = 0.93 ± 0.08 ps), and we therefore assign it to the S_n state of the hexayne. To our knowledge, this is first time that a $S_n \rightarrow S_1$ transition of any polyynes has been characterized by TRIR and NIR TA spectroscopy, although the S_1 and S_n states of the diphenylacetylene were studied by emission spectroscopy.[26,63] π-Conjugated terminal aryl groups may play an important role in the excited-state dynamics of diphenylacetylene, while the "supertrityl" capped hexayne **H** presents a "pure" case of a polyyne chain, so its behavior can be regarded as intrinsic to the sp-hybridized carbyne chain.

Macrocycle M. The excited states of 2,9-diaryl phenanthrolines have been studied before,[57a] and the $^1\pi\pi^*$ singlet-state lifetime is estimated to be a few ns in dichloromethane, while the triplet $^3\pi\pi^*$ state lives for about a second at 77 K. As expected, the TRIR spectrum of macrocycle **M** does not exhibit any features in the high-frequency region (on excitation at 350 or 310 nm). In the fingerprint region, transient features appear at 1470, 1510, and 1520–1600 cm^{-1} (Figure 6a). The transients have similar decay rates, indicating that they arise from the same excited species. The sharpest peak at 1504 cm^{-1} was chosen for kinetic analysis and fitted to a single-exponential decay yielding a singlet lifetime of 2.1 ± 0.2 ns (Figure S6).

The TA spectra show a very broad band between 350 and 700 nm (Figure S7) with distinguishable peaks at 365 and 652 nm. Within a few ns, the peak at 365 nm decays and a new peak grows at 436 nm, but the total intensity of the broad envelope does not change dramatically over time. The decay constant of the 365 nm band is τ_1 = 1.8 ± 0.2 ns, matching with the lifetime of the 1504 cm^{-1} TRIR band. We ascribed the band at 365 nm to the singlet and the band at 436 nm to the triplet excited-state macrocycle.

Rotaxane H⊂M. It is possible to excite the different components of the rotaxane separately: At 350 nm, where only the macrocycle absorbs, or at 310 nm, where absorption by the hexayne predominates (both components absorb at 310 nm, but the molar absorption coefficient of the hexayne is higher by a factor of 12).

The TRIR spectra of **H⊂M**, when excited at 310 nm, are almost identical to those of hexayne **H** (compare Figure 3d–f with Figure 3a–c). The initially formed "hot" S_1 state undergoes rapid energy redistribution, and the observed frequency shift resembles that of the **H** (Figure 3d). The

dx.doi.org/10.1021/ja510663z | J. Am. Chem. Soc. 2014, 136, 17996–18008

bleach of the C≡C stretch around 2190 cm^{-1} does not change intensity during ISC, indicating that the triplet yield is near unity, as in the hexayne **H**. The kinetics are summarized in Table 2. The data from the fingerprint region at late time delays

Table 2. Excited-State Bands, Transitions, and Lifetimes for Rotaxane H⊂M Excited at 310 nm in CH_2Cl_2

TRIR band (cm^{-1})	lifetime (τ)	assignment
2077	0.44 ± 0.02 ns	$S_1 \rightarrow T_1$ decay
2047	0.42 ± 0.05 ns	$S_1 \rightarrow T_1$ growth
1741	0.42 ± 0.01 ns	$S_1 \rightarrow T_1$ decay
1610	0.38 ± 0.02 ns	$S_1 \rightarrow T_1$ growth
2047[a]	0.88 ± 0.04 μs	$T_1 \rightarrow S_0$ decay
1610[a]	1.04 ± 0.05 μs	$T_1 \rightarrow S_0$ decay
1610[a,b]	14.0 ± 2.2 μs	$T_1 \rightarrow S_0$ decay
TA band (nm)	lifetime (τ)	assignment
422	1.8 ± 0.2 ps	$S_n \rightarrow S_1$ growth
422	0.44 ± 0.02 ns	$S_1 \rightarrow T_1$ decay
343	0.55 ± 0.02 ns	$S_1 \rightarrow T_1$ growth

[a]Excited at 266 nm. [b]In O_2-free CH_2Cl_2.

(>15 ps) match those from the high frequency region: the dumbbell S_1 band at 1741 cm^{-1} decays giving rise to a T_1 band at 1610 cm^{-1} (Figure 3f).

Excitation of the rotaxane **H⊂M** at 350 nm, where only the macrocyclic component absorbs, was investigated to test for energy transfer between the two components. (Irradiation of free hexayne **H** at this wavelength does not produce detectable TA and TRIR signals, because **H** has negligible absorption at 350 nm.) On excitation of **H⊂M** at 350 nm, the ground-state C≡C stretch band gradually bleaches, at around 2190 cm^{-1}, and the S_1 polyyne band gradually grows at 2077 cm^{-1} (Figure 3g), indicating transfer of singlet excitation from the macrocycle to the dumbbell. After 20 ps, the TRIR spectra from excitation at 350 nm become identical to those for excitation at 310 nm (compare Figure 3g–i with Figure 3d–f), and the decay kinetics are the same (Figure S1m and Table 3). The spectral

Table 3. Excited-State Bands, Transitions, and Lifetimes for Rotaxane H⊂M Excited at 350 nm in CH_2Cl_2

TRIR band (cm^{-1})	lifetime (τ)	assignment
2077	0.50 ± 0.01 ns ns	$S_1 \rightarrow T_1$ decay
2047	0.44 ± 0.02 ns	$S_1 \rightarrow T_1$ growth
1741	0.48 ± 0.01 ns	$S_1 \rightarrow T_1$ decay
1610	0.45 ± 0.02 ns	$S_1 \rightarrow T_1$ growth
1506	3.2 ± 0.2 ps	EET, S_1 decay of macrocycle
1741	2.7 ± 0.2 ps	EET, S_1 growth of hexayne
TA band (nm)	lifetime (τ)	assignment
422	3.2 ± 0.4 ps	EET, S_1 growth of hexayne
422	0.42 ± 0.04 ns	$S_1 \rightarrow T_1$ decay

changes in the peak at 2060–2080 cm^{-1}, which are observed on a time scale of ∼1 ps upon excitation of **H⊂M** at 310 nm, do not occur when the system is excited at 350 nm (compare Figure 3g with Figure 3d). This difference indicates that the dominant EET process directly populates the S_1 state (without going via the S_n state) and that the early signal is not broadened or shifted by S_n contributions, vibrational energy redistribution or solvent reorganization.

Examination of the fingerprint region of the TRIR spectra of **H⊂M** after excitation at 350 nm showed a fast (<10 ps) decay of a band at 1500–1600 cm^{-1} corresponding to the singlet macrocycle and the parallel rise of the S_1 excited hexayne (1741 cm^{-1}) (Figure 6b). This is direct evidence of singlet–singlet energy transfer from the excited-state macrocycle to the ground-state hexayne. The decay of the macrocycle band at 1560 cm^{-1} (τ_1 = 3.2 ± 0.2 ps) and the growth of the singlet S_1 hexayne at 1741 cm^{-1} (τ_1 = 2.7 ± 0.2 ps) are single-exponential (Figure 6c). The growth of the 2077 cm^{-1} band of the singlet hexayne (τ_1 = 2.6 ± 0.1 ps) and the bleach of the ground-state stretching mode at 2189 cm^{-1} (τ_1 = 2.9 ± 0.3 ps) are also single-exponential. The very weak $S_0 \rightarrow S_1$ oscillation strength of the polyyne implies that this fast EET occurs by a Dexter mechanism. The triplet lifetime of the hexayne component in **H⊂M** (τ_1 = 14.0 ± 2.2 μs in deoxygenated solution, Table 2, Figure S9) is similar to that of the hexayne **H**.

TA spectra of rotaxane **H⊂M**, with excitation at 350 nm, showed formation of a transient S_1 absorption band at 421 nm (Figure 7), similar to that of free dumbbell **H**. The rise-time of

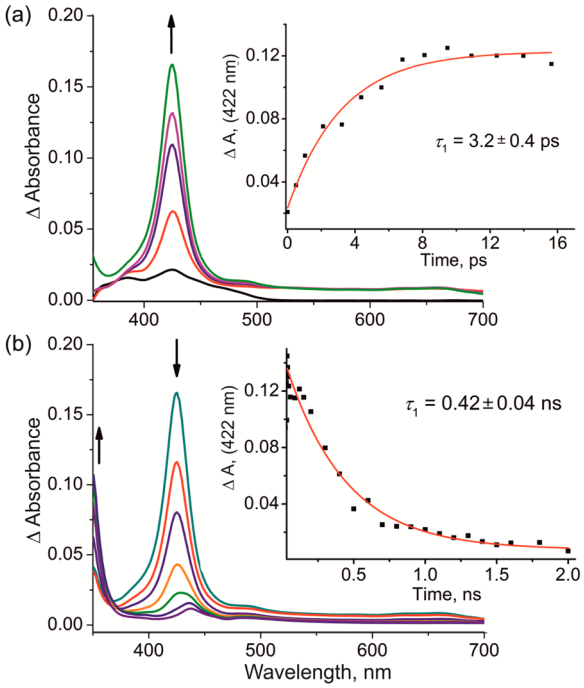

Figure 7. Transient absorption spectra of **H⊂M** following excitation at 350 nm. (a) The formation of singlet excited state. (b) Decrease of singlet and increase of triplet (as a shoulder) TA bands. Inserts show the corresponding kinetics, excited at 350 nm. Laser energy: 200 nJ; solvent: CH_2Cl_2.

this band (τ_1 = 3.2 ± 0.4 ps, Figure 7a), due to S_1(macrocycle) → S_1(hexayne), agrees with the TRIR data. On a longer time scale, this band decays (τ_2 = 0.42 ± 0.04 ns) due to intersystem crossing. The growing T_1 state was observed as a shoulder at 360 nm, but overlap with the excitation wavelength made it difficult to observe the triplet (Figure 7b).

TA spectral changes of **H⊂M** excited at 310 nm are similar to those in dumbbell **H**. The singlet S_1 band at 422 nm grows at early time delays (τ_1 = 1.8 ± 0.2 ps, Figure S10) due to $S_n \rightarrow S_1$ relaxation. Later, this band decays, and the triplet band at 343 nm grows (Figures 5b and S4d and Table 2). The eventual formation of the polyyne triplet state was confirmed by carrying out TA experiments of the rotaxane **H⊂M** in the presence of β-carotene.[64] Excitation of the **H⊂M** at 355 nm resulted in

dx.doi.org/10.1021/ja510663z | J. Am. Chem. Soc. 2014, 136, 17996–18008

triplet−triplet sensitization of the β-carotene (Figure S11). The processes observed by TA and TRIR are summarized in Figure 8.

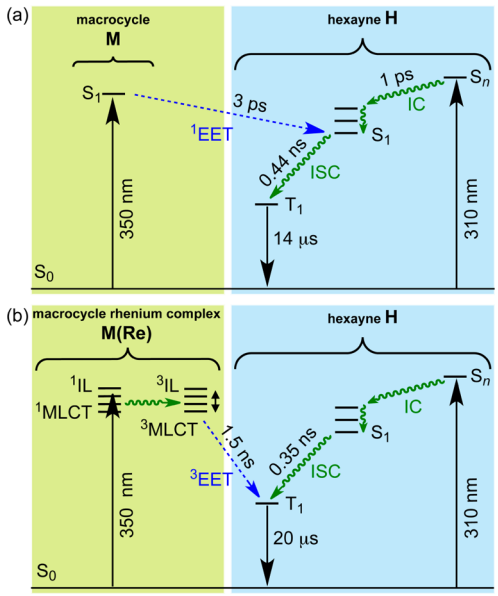

Figure 8. Energy diagram summarizing excited-state processes in (a) dumbbell **H** and rotaxane **H⊂M** and (b) **M(Re)** and $Re(CO)_3Cl$·rotaxane complex **H⊂M(Re)**.

*$Re(CO)_3Cl$-Macrocycle Complex **M(Re)**.* The excited-state dynamics of 1,10-phenanthroline-based $Re(CO)_3Cl$ complexes have been thoroughly described in the literature[57,65] and will only be outlined briefly here for discussion of changes when part of the rotaxane. Optical excitation creates both ^{1}IL and ^{1}MLCT states that undergo intersystem crossing to at least two thermally equilibrating, "hot", triplet ^{3}IL and ^{3}MLCT states, over ∼150 fs. The IL state arises from phenanthroline $\pi-\pi^*$ transition, and the MLCT state also involves the d orbitals of Re atom. Internal conversion between the ^{3}IL and ^{3}MLCT states takes place on a time scale of ps to ns, depending on the solvent and ligand structure. Later, the ^{3}MLCT state relaxes to the vibrationally cooled lowest excited state, which decays on the ns time-scale via radiative and nonradiative pathways.[66]

On excitation of **M(Re)** at 350 nm, TRIR spectra show several positive bands from photogenerated species as well as negative bands originating from the depleted ground state (Figure 9a). Recent 2D-IR studies by Bredenbeck et al.[66e] indicate that the order of the bands in the excited state is different from that in the ground state; bands were observed at 1944, 1985, and 2048 cm^{-1} due to A″, A′(2), and A′(1) modes, respectively, and we adopt this assignment. The broad positive band at 1935−2005 cm^{-1} represents the overlap of A″ and A′(2) excited-state bands.[66d,67] The time-dependent shift of these two bands is complex, as it incorporates the instantaneous shift, as a result of Franck−Condon excitation and formation of an excited state of mixed ^{3}IL and ^{3}MLCT character stemming from combined $d\pi \rightarrow \pi^*$ and $\pi \rightarrow \pi^*$ excitation. In addition, all of these processes are accompanied by solvent reorganization.[66,67] Over 10 ps, the low-energy shoulder of the excited-state A″ band decreases. The higher energy weak shoulder next to the excited-state A′(2) band also decreases over 10 ps. The A″ band undergoes a ∼17 cm^{-1} shift to higher frequency with a 26% intensity increase, while the ground-state A″ band bleach increases by 22%. The bleach and transient intensity changes can be attributed to changes in the relative intensity of overlapping TA bands, as the character of the ^{3}IL/^{3}MLCT state evolves at early times, with the ^{3}MLCT becoming dominant.[66a] The A′(1) excited band at 2054 cm^{-1} shows a more pronounced intensity increase (62%), hypsochromic shift (12 cm^{-1}), and band narrowing (64%) (Figure 9a). Whereas the shift to higher frequency is due to an increasing contribution of the ^{3}MLCT state,[67a] the band-narrowing apparently involves vibrational relaxation steps, stemming from local-solvent reorganization. These spectral changes resemble the excited-state dynamics of the $Re(CO)_3$(4-Et-pyridine) 2,2′-bipyridine complex.[68] We ascribe the final TRIR spectral pattern, seen at longer time delays, to the relaxed lowest excited-state triplet (see Figure 8 for a summary of the excited states and kinetics). Kinetic data were extracted from TRIR spectra, exciting **M(Re)** at 266 nm, so as to estimate the lifetime of the triplet excited state. All negative and positive bands show similar single-exponential kinetics. The triplet lifetime is 93 ns under oxygen-free conditions (Figure S12) and 63 ns in the presence of air (Figure 9b, Table S1).

In the fingerprint region of the TRIR spectrum of **M(Re)**, two bleaches of ground-state bands at 1497 and 1608 cm^{-1} appear immediately after excitation, and recover within ∼30−40 ps, while the transient bands 1480 and 1595 cm^{-1} grow slightly (Figure 9c). The positions of the bleach bands in **M(Re)** and **M** are similar, suggesting that they originate from the phenanthroline framework, and are not strongly perturbed by the presence of the rhenium. Furthermore, in **M(Re)**, the recovery of these bleach bands is partial, due to overlapping positive bands, and shows single-exponential recovery kinetics (1497 cm^{-1}: τ_1 = 6.8 ± 0.6 ps; 1608 cm^{-1}: τ_1 = 14.0 ± 1.2 ps; Figure S13d), on a time scale similar to the ν(CO) shifts observed in the transients in the carbonyl stretching region. Thus, we tentatively assign the bleach recovery at 1497 and 1608 cm^{-1} to the cooling and molecular reorganization processes of the initially formed unrelaxed states.

*$Re(CO)_3Cl$-Rotaxane Complex **H⊂M(Re)**.* The ground-state CO and C≡C stretch vibrations of **H⊂M(Re)** occur at different frequencies, allowing each component to be observed separately. TRIR spectra of **H⊂M(Re)** following excitation of the macrocycle component at 350 nm show immediate bleaching of ground-state carbonyl stretching bands (Figure S14). The excited-state CO bands at 2051 and 1975 cm^{-1} shift to high frequencies within 20 ps, due to the ^{3}IL → ^{3}MLCT conversion and vibration relaxation, as in **M(Re)**. However, in contrast to **M(Re)**, the CO bleaches of **H⊂M(Re)** undergo rapid recovery (Figure 9d,e). The recovery of the CO bleach is accompanied by bleaching of the C≡C band at ∼2190 cm^{-1}, indicating energy transfer from $Re(CO)_3Cl$·macrocycle to the hexayne chain. The rate of C≡C bleaching matches that of the recovery of all three CO bands (Figure 9e). Kinetic data are summarized in Table 4. The TRIR spectra of **H⊂M(Re)** in the high-frequency region do not reveal the nature of energy transfer, as the triplet and singlet-state bands of the hexayne at 2040−2080 cm^{-1} overlap with excited-state A′(1) band. The necessary information was obtained from the fingerprint region: the initial bleach of the excited $Re(CO)_3Cl$·macrocycle at 1607 cm^{-1} recovers, and then the band corresponding to the triplet-state hexayne at ca. 1610 cm^{-1} grows over 2 ns (Figures 9f and S13). At the same time the triplet $Re(CO)_3Cl$·macrocycle band around 1470 cm^{-1} decays (τ_1 = 1.86 ± 0.15 ns). These spectral

dx.doi.org/10.1021/ja510663z | J. Am. Chem. Soc. 2014, 136, 17996−18008

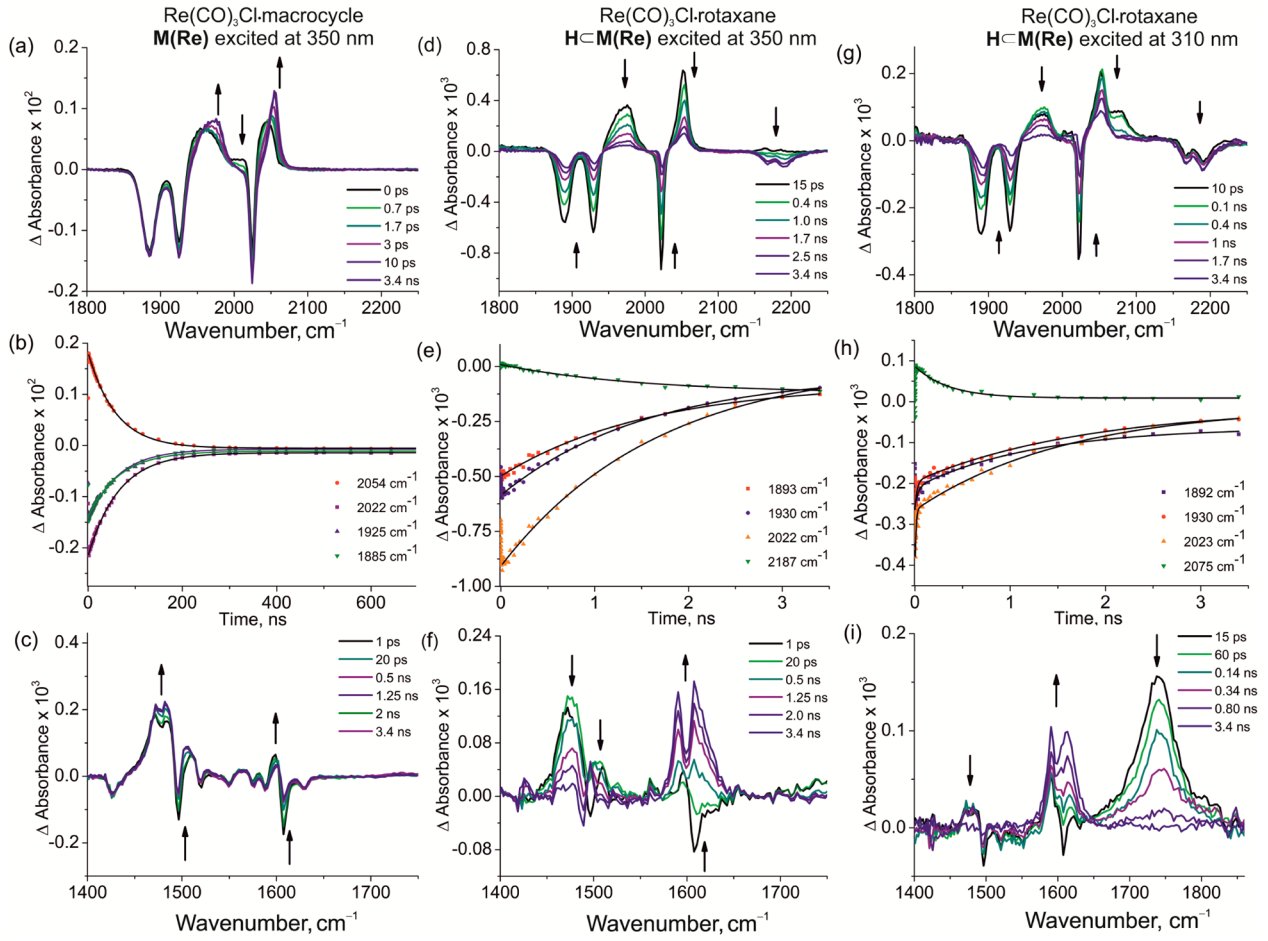

Figure 9. TRIR spectra and excited-state kinetics of the **M(Re)** (a–c) excited at 350 nm, **H⊂M(Re)** excited at 350 nm (d–f), and 310 nm (g–i). Laser energy: 100–200 nJ; solvent: CH_2Cl_2.

Table 4. Excited-State Bands, Transitions, and Lifetimes for H⊂M(Re) Excited at 350 nm in CH_2Cl_2

TRIR band (cm^{-1})	lifetime (τ)	assignment
1470	1.86 ± 0.15 ns	^{3}EET, T_1 decay of macrocycle
1610	14.0 ± 0.6 ps (A_1 = 0.35)	relaxation
	1.10 ± 0.05 ns (A_2 = 0.65)	^{3}EET, growth of T_1 polyyne
1892	1.59 ± 0.12 ns	νCO_{gs} bleach (decaying); ^{3}EET
1930	1.50 ± 0.11 ns	
2022	1.70 ± 0.09 ns	
2185	1.44 ± 0.12 ns	$\nu C{\equiv}C$ bleach (growing); ^{3}EET
1610[a]	20.2 ± 1.7 μs	polyyne $T_1 \rightarrow S_0$ decay

[a]Excited at 266 nm and measured in O_2-free CH_2Cl_2.

changes clearly demonstrate triplet–triplet energy transfer from the $Re(CO)_3Cl$·macrocycle moiety to the threaded hexayne.

The growth kinetics of the 1607 cm^{-1} band (Figure S13h) are biexponential (τ_1 = 14.0 ± 0.6 ps, A_1 = 0.35; τ_2 = 1.13 ± 0.05 ns, A_2 = 0.65) with the fast component matching that of decay of the bleach at 1607 cm^{-1} in $Re(CO)_3Cl$·macrocycle **M(Re)**. This implies that in excited **H⊂M(Re)**, ^{3}IL/^{3}MLCT relaxation, vibrational cooling, and solvent reorganization take place in parallel with triplet energy transfer to the hexayne from a relaxed ^{3}MLCT state. Indeed, the hexayne ground-state C≡C band at ~2200 cm^{-1} does not show any bleach over the first 20–30 ps, while the ^{3}IL/^{3}MLCT and other relaxations take place (Figures 9f and S14).

The TRIR spectra of **H⊂M(Re)** using excitation at 350 nm did not show any singlet excited-state polyyne band, before or after energy transfer, excluding the possibility of singlet energy transfer from the $Re(CO)_3Cl$·macrocycle. Singlet energy transfer does not occur because intersystem crossing in the $Re(CO)_3Cl$·macrocycle complex is ultrafast, and all spectral changes originate from triplet excited $Re(CO)_3Cl$·macrocycle. Thus, triplet sensitization of the hexayne in **H⊂M(Re)** upon excitation of the molecule at 350 nm explains the quenching of emission of $Re(CO)_3Cl$·macrocycle **M(Re)** at room temperature by the threaded dumbbell.[16] The efficiency of ^{3}EET was estimated by comparing the intensities of the C≡C band at ~2200 cm^{-1} and the A′(1) C═O at 2054 cm^{-1} in the ground-state IR spectra and in the TRIR spectra, at the time of maximum bleach (Figure S15). This analysis indicates that the efficiency of ^{3}EET is $\Phi_{EET} \geq 99\%$.

Another noteworthy feature of the **H⊂M(Re)** rotaxane is the perturbation of the ground-state hexayne by excited **M(Re)** (after excitation, before energy transfer) which appears as a slightly enhanced absorption at ~2200 cm^{-1} (Figures 9d and S16). Later, when **M(Re)** is in its relaxed state, after EET, the carbonyl bleaches do not decay to zero, although all positive transient bands disappear (Figure S16) as a result of electronic perturbation by the nearby triplet hexayne. In both cases, this effect serves to report the presence of a nearby excited-state

dx.doi.org/10.1021/ja510663z | J. Am. Chem. Soc. 2014, 136, 17996–18008

constituent. The triplet-state polyyne lifetimes in deoxygenated and oxygen-containing solutions (Figure S17) are similar to those of the rotaxane **H⊂M** (Table 2). These processes are summarized in Figure 8b.

Direct excitation of the hexayne component of **H⊂M(Re)** at 310 nm generates the singlet-state hexayne via direct excitation as well as triplet macrocycle (Figure 2a) followed by triplet energy transfer to the hexayne. In Figure 9g, for example, the band around 2070 cm^{-1}, corresponding to singlet hexayne, decreases gradually (τ_1 = 0.35 ± 0.03 ns), while the C≡C bleach, which appeared immediately upon excitation, increases (~2200 cm^{-1}) due to triplet energy transfer from macrocycle to hexayne. Upon triplet EET the excited macrocycle bands also decrease and the ν(CO) bleach recovers (Figure S13, Table S1). Comparable changes are observed in the fingerprint region (Figure 9i) where the singlet hexayne band at 1741 cm^{-1} decreases and triplet band at 1610 cm^{-1} increases. Kinetic analysis of the fingerprint region shows that the singlet hexayne band at 1741 cm^{-1} decays in a single-exponential fashion (Figure S13, τ_1 = 0.35 ± 0.01 ns); the decay constant matches that of the singlet band at 2070 cm^{-1}.

TA spectra of **H⊂M(Re)** excited at 310 nm show the formation of singlet and triplet excited states similar to rotaxane **H⊂M** and hexayne **H** excited at 310 nm (Figure 5a,b). Within 5 ps the band of the singlet hexayne at 422 nm grows over the broad transient envelope band of the macrocycle (Figure S18). The singlet-state band at 422 nm decays single-exponentially with τ_1 = 0.34 ± 0.01 ps. The broad band of the macrocycle also decreases, and the growth of hexayne triplet band at 343 nm is single exponential (τ_2 = 0.49 ± 0.02 ns, Figure S4f). Both τ_1 and τ_2 values agree with the TRIR data. The kinetic data are summarized in Tables 4 and S1.

Calculated IR Spectra of Hexayne S_0, S_1, and T_1 States. We calculated the IR spectra of a model hexayne (Me−C_{12}−Me) in its ground and excited states, to gain insights into the structural changes in the electronic excited states that are responsible for the observed TRIR bands of hexayne **H**. In particular, we sought to understand why the experimental S_1 and T_1 spectra each exhibit one vibration in the fingerprint region (1500−1900 cm^{-1}) and one vibration in the high-frequency region (2000−2250 cm^{-1}). Symmetric polyynes have been thoroughly studied by Raman spectroscopy,[29,56,59] but few investigations of their IR spectra have been reported.[40,60] Details of our computational methodology are given above. The combined computational and experimental results provide compelling evidence for cumulenic character in the S_1 and T_1 electronic states of **H**.

The calculated bond lengths of the S_0, S_1, and T_1 states (Figures 10 and S19) reveal a reduction in bond length alternation in S_1 and T_1, compared with S_0, indicating that the excited states have significant cumulenic character, particularly near the center of the chain. These results agree well with previous work,[28,30,37−40,54i] and the calculated bond lengths in the S_0 are close to those from the crystal structure of **H**.[9]

The presence of two CC excited-state bonding regions (quasi-acetylenic at the ends and quasi-cumulenic in the middle) is supported by the experimental and calculated vibrational spectra. Within the spectral region of interest (1500−2250 cm^{-1}), the calculated spectra show remarkable agreement with the experimental TRIR data (Figure 11). The S_0 vibrational spectrum shows two bands, ν_2 (calculated: 2172 cm^{-1}; observed: 2165 cm^{-1}) and ν_1 (calculated: 2207 cm^{-1}; observed: 2191 cm^{-1}). For S_1 and T_1, the calculated frequencies

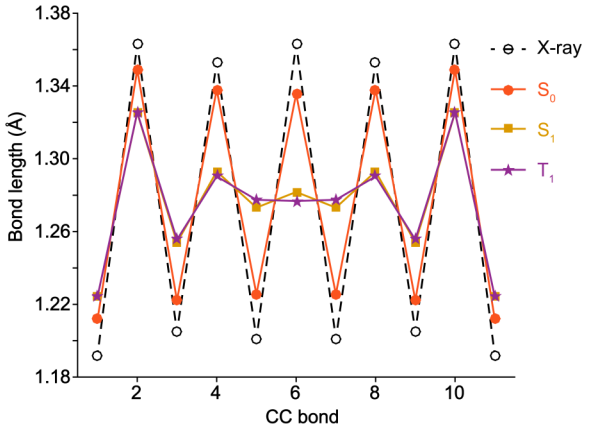

Figure 10. Bond length alternation in **H** (from crystallographic data, black circles; ref 9) and in calculated (B3LYP/cc-pVTZ) S_0 (red circles), S_1 (yellow squares), and T_1 (purple stars) states.

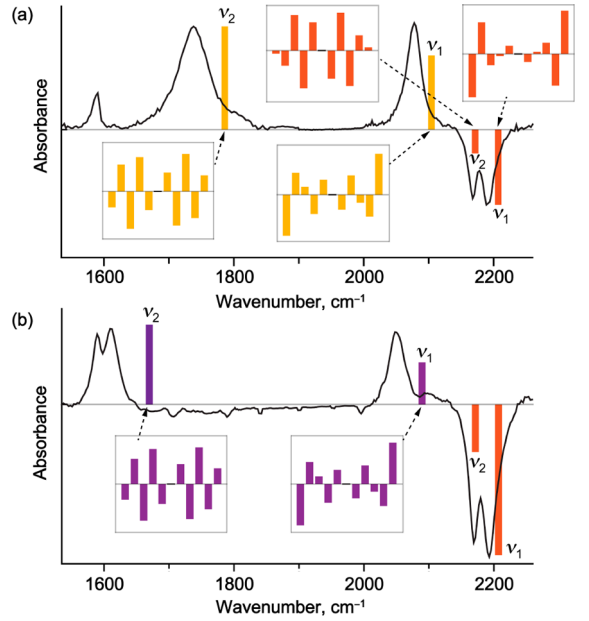

Figure 11. Calculated IR spectra for Me-C_{12}-Me (bars) and experimental TRIR spectra for **H** (lines) (a) 20 ps after excitation (S_1) and (b) 3.4 ns after excitation (T_1). Red, yellow, and purple bars denote calculated (B3LYP/cc-pVTZ) frequencies for S_0, S_1, and T_1 states, respectively. Inset plots show bond length displacements for each of the indicated IR modes of the C_{12} chain, the change in bond length being proportional to the direction and magnitude of the bar.

agree with experiment and predict a ν_1 band in the C≡C region (S_1: 2104 cm^{-1}; T_1: 2089 cm^{-1}), and a lower energy ν_2 band in the fingerprint region (S_1: 1786 cm^{-1}; T_1: 1670 cm^{-1}). On the basis of the match between the calculated and observed spectra, we assign the ν_1 and ν_2 bands to asymmetric stretch vibrations of the C≡C chain, as shown in the insets in Figures 11 and S19. The patterns of atomic displacement for both modes of S_1 and T_1 show close correspondence, as expected given the similar bonding in these two states (Figure 10).

The large change in frequency of the ν_2 mode (in contrast to ν_1) in the excited states (S_1 and T_1), compared with the S_0 ground state, can be rationalized by considering the nature of the vibrational modes. For each electronic state, the higher energy ν_1 vibration involves greater displacement of the CC bonds at the ends of the hexayne, whereas the lower energy ν_2

dx.doi.org/10.1021/ja510663z | J. Am. Chem. Soc. 2014, 136, 17996−18008

vibration involves displacement of bonds near the center (insets in Figures 11 and S19), making it much more sensitive to the excited-state cumulenic character around the center of the molecule.

CONCLUSION

Despite the alluring elemental simplicity of their molecular structures, polyyne chromophores exhibit remarkably rich and complex photophysical behavior. Here we have shown that TRIR, coupled with DFT calculations, is an excellent technique for probing their excited-state dynamics. We have also demonstrated that rotaxane synthesis is a powerful strategy for fixing a photoactive unit near the center of a polyyne chain, for studying singlet and triplet energy-transfer through-space, between nonbonded components. Previously it was found that butadiyne bridges can mediate quantitative intramolecular triplet EET between covalently bonded chromophores.[69] Here we demonstrate the intermolecular triplet EET properties of polyynes in a covalently nonbonded rotaxane. The singlet and triplet excitation energy harvesting properties of polyynes resemble those of the carotenes, which harvest both triplet and singlet energy in photosynthetic systems.[70] It is intriguing to consider why nature exclusively preferred conjugated double rather triple bonds for photosynthetic energy transfer. Understanding the excited states of polyyne in supramolecular assemblies, such as the rotaxane studied here, is important for further application of materials based on chains of linear sp carbon atoms in molecular and optoelectronic devices.[1] This study demonstrates how the photochemistry of a system can be controlled through nonbonded interactions, without altering the chromophore or relying on diffusion, through synthesis of rotaxane architectures.

ASSOCIATED CONTENT

Supporting Information

Supplementary TRIR and TA spectra, further details on DFT calculations, and calculated geometries. This material is available free of charge via the Internet at http://pubs.acs.org.

AUTHOR INFORMATION

Corresponding Authors

harry.anderson@chem.ox.ac.uk
tony.parker@stfc.ac.uk

Notes

The authors declare no competing financial interest.

ACKNOWLEDGMENTS

We thank Rik R. Tykwinski (Erlangen) and Daniele Fazzi (MPI, Mülheim) for valuable discussion, STFC for access to the Central Laser Facility - RCaH (12,230,011 and 1120009), the European Research Council (ERC) for funding, the Advanced Research Computing (ARC) facility (Oxford) for provision of computational facilities, and Diamond Light Source for a generous award of beamtime on I19 (MT9981) and the instrument scientists for support. L.D.M. acknowledges Oxford University Raffy Manoukian scholarship for financial support.

REFERENCES

(1) (a) Diederich, F.; Rubin, Y. *Angew. Chem., Int. Ed. Engl.* **1992**, *31*, 1101. (b) Diederich, F. *Nature* **1994**, *363*, 199. (c) *Acetylene Chemistry: Chemistry, Biology, and Material Science*; Diederich, F., Stang, P. J., Tykwinski, R. R., Eds.; Wiley-VCH: Weinheim, Germany, 2005. (d) Chalifoux, W. A.; Tykwinski, R. R. *C. R. Chim.* **2009**, *12*, 341. (e) Diederich, F.; Kivala, M. *Adv. Mater.* **2010**, *22*, 803. (f) Januszewski, J. A.; Tykwinski, R. R. *Chem. Soc. Rev.* **2014**, *43*, 3184. (g) Chernick, E. T.; Tykwinski, R. R. *J. Phys. Org. Chem.* **2013**, *26*, 742.

(2) (a) Itzhaki, L.; Altus, E.; Basch, H.; Hoz, S. *Angew. Chem., Int. Ed.* **2005**, *44*, 7432. (b) Liu, M.; Artyukhov, V. I.; Lee, H.; Xu, F.; Yakobson, B. I. *ACS Nano* **2013**, *7*, 10075.

(3) (a) Wang, C.; Batsanov, A. S.; Bryce, M. R.; Martín, S.; Nichols, R. J.; Higgins, S. J.; García-Suárez, V. M.; Lambert, C. J. *J. Am. Chem. Soc.* **2009**, *131*, 15647. (b) Moreno-García, P.; Gulcur, M.; Manrique, D. Z.; Pope, T.; Hong, W.; Kaliginedi, V.; Huang, C.; Batsanov, A. S.; Bryce, M. R.; Lambert, C.; Wandlowski, T. *J. Am. Chem. Soc.* **2013**, *135*, 12228.

(4) Vail, S. A.; Krawczuk, P. J.; Guldi, D. M.; Palkar, A.; Echegoyen, L.; Tomé, J. P. C.; Fazio, M. A.; Schuster, D. I. *Chem.—Eur. J.* **2005**, *11*, 3375.

(5) (a) Cretu, O.; Botello-Mendez, A. R.; Janowska, I.; Pham-Huu, C.; Charlier, J.-C.; Banhart, F. *Nano Lett.* **2013**, *13*, 3487. (b) Al-Backri, A.; Zólyomi, V.; Lambert, C. J. *J. Chem. Phys.* **2014**, *140*, 104306.

(6) Cao, Z.; Xi, B.; Jodoin, D. S.; Zhang, L.; Cummings, S. P.; Gao, Y.; Tyler, S. F.; Fanwick, P. E.; Crutchley, R. J.; Ren, T. *J. Am. Chem. Soc.* **2014**, *136*, 12174.

(7) (a) Slepkov, A. D.; Hegmann, F. A.; Eisler, S.; Elliott, E.; Tykwinski, R. R. *J. Chem. Phys.* **2004**, *120*, 6807. (b) Eisler, S.; Slepkov, A. D.; Elliott, E.; Luu, T.; McDonald, R.; Hegmann, F. A.; Tykwinski, R. R. *J. Am. Chem. Soc.* **2005**, *127*, 2666. (c) Samoc, M.; Dalton, G. T.; Gladysz, J. A.; Zheng, Q.; Velkov, Y.; Ågren, H.; Norman, P.; Humphrey, M. G. *Inorg. Chem.* **2008**, *47*, 9946.

(8) Schrettl, S.; Stefaniu, C.; Schwieger, C.; Pasche, G.; Oveisi, E.; Fontana, Y.; Fontcuberta i Morral, A.; Reguera, J.; Petraglia, R.; Corminboeuf, C.; Brezesinski, G.; Frauenrath, H. *Nat. Chem.* **2014**, *6*, 468.

(9) Chalifoux, W. A.; Tykwinski, R. R. *Nat. Chem.* **2010**, *2*, 967.

(10) Zhao, C.; Kitaura, R.; Hara, H.; Irle, S.; Shinohara, H. *J. Phys. Chem. C* **2011**, *115*, 13166.

(11) Weller, M. D.; Cox, L. R. *C. R. Chim.* **2009**, *12*, 366.

(12) Taylor, T. J.; Gabbaï, F. P. *Organometallics* **2006**, *25*, 2143.

(13) (a) Stahl, J.; Bohling, J. C.; Bauer, E. B.; Peters, T. B.; Mohr, W.; Martin-Alvarez, J. M.; Hampel, F.; Gladysz, J. A. *Angew. Chem., Int. Ed.* **2002**, *41*, 1871. (b) de Quadras, L.; Bauer, E. B.; Mohr, W.; Bohling, J. C.; Peters, T. B.; Martín-Alvarez, J. M.; Hampel, F.; Gladysz, J. A. *J. Am. Chem. Soc.* **2007**, *129*, 8296.

(14) Peck, E. M.; Collins, C. G.; Smith, B. D. *Org. Lett.* **2013**, *15*, 2762.

(15) (a) Frampton, M. J.; Anderson, H. L. *Angew. Chem., Int. Ed.* **2007**, *46*, 1028. (b) Yau, C. M. S.; Pascu, S. I.; Odom, S. A.; Warren, J. E.; Klotz, E. J. F.; Frampton, M. J.; Williams, C. C.; Coropceanu, V.; Kuimova, M. K.; Phillips, D.; Barlow, S.; Brédas, J.-L.; Marder, S. R.; Millar, V.; Anderson, H. L. *Chem. Commun.* **2008**, 2897. (c) Sforazzini, G.; Kahnt, A.; Wykes, M.; Sprafke, J. K.; Brovelli, S.; Montarnal, D.; Meinardi, F.; Cacialli, F.; Beljonne, D.; Albinsson, B.; Anderson, H. L. *J. Phys. Chem. C* **2014**, *118*, 4553.

(16) Movsisyan, L. D.; Kondratuk, D. V.; Franz, M.; Thompson, A. L.; Tykwinski, R. R.; Anderson, H. L. *Org. Lett.* **2012**, *14*, 3424.

(17) (a) Weisbach, N.; Baranová, Z.; Gauthier, S.; Reibenspies, J. H.; Gladysz, J. A. *Chem. Commun.* **2012**, *48*, 7562. (b) Sahnoune, H.; Baranová, Z.; Bhuvanesh, N.; Gladysz, J. A.; Halet, J.-F. *Organometallics* **2013**, *32*, 6360.

(18) Saito, S.; Nakazono, K.; Takahashi, E. *J. Org. Chem.* **2006**, *71*, 7477.

(19) Lo, K. K.-W.; Louie, M.-W.; Zhang, K. Y. *Coord. Chem. Rev.* **2010**, *254*, 2603.

(20) Cleland, D. M.; Irwin, G.; Wagner, P.; Officer, D. L.; Gordon, K. C. *Chem.—Eur. J.* **2009**, *15*, 3682.

(21) Vlček, A., Jr. *Top. Organomet. Chem.* **2010**, *29*, 73.

(22) Kumar, A.; Sun, S.-S.; Lees, A. J. *Top. Organomet. Chem.* **2010**, *29*, 1.

(23) Gibtner, T.; Hampel, F.; Gisselbrecht, J.-P.; Hirsch, A. *Chem.—Eur. J.* **2002**, *8*, 408.
(24) Wright, P. J.; Muzzioli, S.; Werrett, M. V.; Raiteri, P.; Skelton, B. W.; Silvester, D. S.; Stagni, S.; Massi, M. *Organometallics* **2012**, *31*, 7566.
(25) (a) George, M. W.; Turner, J. J. *Coord. Chem. Rev.* **1998**, *177*, 201. (b) Butler, J. M.; George, M. W.; Schoonover, J. R.; Dattelbaum, D. M.; Meyer, T. J. *Coord. Chem. Rev.* **2007**, *251*, 492.
(26) TRIR studies of diphenylacetylene have been reported: (a) Ishibashi, T.; Okamoto, H.; Hamaguchi, H. *Chem. Phys. Lett.* **2000**, *325*, 212. (b) Nomoto, T.; Ishibashi, T.; Okamoto, H.; Hamaguchi, H. *J. Mol. Str.* **2005**, *735*−*736*, 197.
(27) Kloster-Jensen, E.; Haink, H.-J.; Christen, H. *Helv. Chim. Acta* **1974**, *57*, 1731.
(28) Pino, T.; Ding, H.; Güthe, F.; Maier, J. P. *J. Chem. Phys.* **2001**, *114*, 2208.
(29) Wakabayashi, T.; Nagayama, H.; Daigoku, K.; Kiyooka, Y.; Hashimoto, K. *Chem. Phys. Lett.* **2007**, *446*, 65.
(30) Wakabayashi, T.; Wada, Y.; Iwahara, N.; Sato, T. *J. Phys.: Conf. Ser.* **2013**, *428*, 012004.
(31) Eastmond, R.; Johnson, T. R.; Walton, D. R. M. *Tetrahedron* **1972**, *28*, 4601.
(32) (a) Hirata, Y.; Okada, T.; Nomoto, T. *Chem. Phys. Lett.* **1998**, *293*, 371. (b) Saltiel, J.; Kumar, V. K. R. *J. Phys. Chem. A* **2012**, *116*, 10548.
(33) (a) Nagano, Y.; Ikoma, T.; Akiyama, K.; Tero-Kubota, S. *J. Chem. Phys.* **2001**, *114*, 1775. (b) Nagano, Y.; Ikoma, T.; Akiyama, K.; Tero-Kubota, S. *J. Am. Chem. Soc.* **2003**, *125*, 14103.
(34) Simpkins, S. M. E.; Weller, M. D.; Cox, L. R. *Chem. Commun.* **2007**, 4035.
(35) Deperasińska, I.; Szemik-Hojniak, A.; Osowska, K.; Rode, M. F.; Szczepanik, A.; Wiśniewski, Ł.; Lis, T.; Szafert, S. *J. Photochem. Photobiol., A* **2011**, *217*, 299.
(36) Fazzi, D.; Scotognella, F.; Milani, A.; Brida, D.; Manzoni, C.; Cinquanta, E.; Devetta, M.; Ravagnan, L.; Milani, P.; Cataldo, F.; Lüer, L.; Wannemacher, R.; Cabanillas-Gonzalez, J.; Negro, M.; Stagira, S.; Vozzi, C. *Phys. Chem. Chem. Phys.* **2013**, *15*, 9384.
(37) Haque, M.; Yin, L.; Nugraha, A. R. T.; Saito, R. *Carbon* **2011**, *49*, 3340.
(38) Karpfen, A.; Liscka, H. *Chem. Phys.* **1986**, *102*, 91.
(39) Yoneda, H.; Hiura, H.; Takahashi, H. *J. Mol. Struct.* **1993**, *301*, 47.
(40) (a) Yildizhan, M. M.; Fazzi, D.; Milani, A.; Brambilla, L.; Zoppo, M. D.; Chalifoux, W. A.; Tykwinski, R. R.; Zerbi, G. *J. Chem. Phys.* **2011**, *134*, 124512. (b) Lucotti, A.; Tommasini, M.; Chalifoux, W. A.; Fazzi, D.; Zerbi, G.; Tykwinski, R. R. *J. Raman Spectrosc.* **2012**, *43*, 95.
(41) Nowell, H.; Barnett, S. A.; Christensen, K. E.; Teat, S. J.; Allan, D. R. *J. Synch. Rad.* **2012**, *19*, 435.
(42) (a) Palatinus, L.; van der Lee, A. *J. Appl. Crystallogr.* **2008**, *41*, 975. (b) Palatinus, L. *Acta Crystallogr.* **2013**, *B69*, 1.
(43) Palatinus, L.; Chapuis, G. *J. Appl. Crystallogr.* **2007**, *40*, 786.
(44) (a) Betteridge, P. W.; Carruthers, J. R.; Cooper, R. I.; Prout, K.; Watkin, D. J. *J. Appl. Crystallogr.* **2003**, *36*, 1487. (b) Cooper, R. I.; Thompson, A. L.; Watkin, D. J. *J. Appl. Crystallogr.* **2010**, *43*, 1100.
(45) (a) Spek, A. *J. Appl. Crystallogr.* **2003**, *36*, 7. (b) van der Sluis, P.; Spek, A. L. *Acta Crystallogr.* **1990**, *A46*, 194.
(46) Greetham, G. M.; Burgos, P.; Cao, Q.; Clark, I. P.; Codd, P. S.; Farrow, R. C.; George, M. W.; Kogimtzis, M.; Matousek, P.; Parker, A. W.; Pollard, M. R.; Robinson, D. A.; Xin, Z.-J.; Towrie, M. *Appl. Spectrosc.* **2010**, *64*, 1311.
(47) TURBOMOLE V6.1 (2009), a development of University of Karlsruhe and Forschungszentrum Karlsruhe GmbH, 1989−2007, TURBOMOLE GmbH, since 2007; available from http://www.turbomole.com; Ahlrichs, R.; Bär, M.; Häser, M.; Horn, H.; Kölmel, C. *Chem. Phys. Lett.* **1989**, *162*, 165.
(48) (a) Becke, A. D. *J. Chem. Phys.* **1993**, *98*, 5648. (b) Lee, C.; Yang, W.; Parr, R. G. *Phys. Rev. B* **1988**, *37*, 785.
(49) (a) Perdew, J. P.; Burke, K.; Ernzerhof, M. *Phys. Rev. Lett.* **1996**, *77*, 3865. (b) Perdew, J. P.; Ernzerhof, M.; Burke, K. *J. Chem. Phys.* **1996**, *105*, 9982.
(50) (a) Sierka, M.; Hogekamp, A.; Ahlrichs, R. *J. Chem. Phys.* **2003**, *118*, 9136. (b) Deglmann, P.; May, K.; Furche, F.; Ahlrichs, R. *Chem. Phys. Lett.* **2004**, *384*, 103. (c) Eichkorn, K.; Treutler, O.; Öhm, H.;. (d) Häser, M.; Ahlrichs, R. *Chem. Phys. Lett.* **1995**, *242*, 652. (e) Eichkorn, K.; Weigend, F.; Treutler, O.; Ahlrichs, R. *Theor. Chem. Acc.* **1997**, *97*, 119. (f) Weigend, F. *Phys. Chem. Chem. Phys.* **2006**, *8*, 1057.
(51) Rowland, R. S.; Taylor, R. *J. Phys. Chem.* **1996**, *100*, 7384.
(52) Szafert, S.; Gladysz, J. A. *Chem. Rev.* **2006**, *106*, PR1.
(53) Allen, F. H. *Acta Crystallogr.* **2002**, *B58*, 380.
(54) (a) Sakurai, A.; Akita, M.; Moro-oka, Y. *Organometallics* **1999**, *18*, 3241. (b) Peters, T. B.; Bohling, J. C.; Arif, A. M.; Gladysz, J. A. *Organometallics* **1999**, *18*, 3261. (c) Adams, R. D.; Qu, B.; Smith, M. D. *Organometallics* **2002**, *21*, 3867. (d) Classen, J.; Gleiter, R.; Rominger, F. *Eur. J. Inorg. Chem.* **2002**, 2040. (e) Mohr, W.; Stahl, J.; Hampel, F.; Gladysz, J. A. *Chem.—Eur. J.* **2003**, *9*, 3324. (f) Qi, H.; Gupta, A.; Noll, B. C.; Snider, G. L.; Lu, Y.; Lent, C.; Fehlner, T. P. *J. Am. Chem. Soc.* **2005**, *127*, 15218. (g) Luu, T.; Elliott, E.; Slepkov, A. D.; Eisler, S.; McDonald, R.; Hegmann, F. A.; Tykwinski, R. R. *Org. Lett.* **2005**, *7*, 51. (h) Bruce, M. I.; Zaitseva, N. N.; Nicholson, B. K.; Skelton, B. W.; White, A. H. *J. Organomet. Chem.* **2008**, *693*, 2887. (i) Lucotti, A.; Tommasini, M.; Fazzi, D.; Del Zoppo, M.; Chalifoux, W. A.; Ferguson, M. J.; Zerbi, G.; Tykwinski, R. R. *J. Am. Chem. Soc.* **2009**, *131*, 4239. (j) Frank, B. B.; Kivala, M.; Blanco, B. C.; Breiten, B.; Schweizer, W. B.; Laporta, P. R.; Biaggio, I.; Jahnke, E.; Tykwinski, R. R.; Boudon, C.; Gisselbrecht, J.-P.; Diederich, F. *Eur. J. Org. Chem.* **2010**, 2487. (k) Gulia, N.; Osowska, K.; Pigulski, B.; Lis, T.; Galewski, Z.; Szafert, S. *Eur. J. Org. Chem.* **2012**, 4819.
(55) Mohr, W.; Stahl, J.; Hampel, F.; Gladysz, J. A. *Inorg. Chem.* **2001**, *40*, 3263.
(56) Wakabayashi, T.; Tabata, H.; Doi, T.; Nagayama, H.; Okuda, K.; Umeda, R.; Hisaki, I.; Sonoda, M.; Tobe, Y.; Minematsu, T.; Hashimoto, K.; Hayashi, S. *Chem. Phys. Lett.* **2007**, *433*, 296.
(57) (a) Armaroli, N.; De Cola, L.; Balzani, V.; Sauvage, J.-P.; Dietrich-Buchecker, C. O.; Kern, J.-M. *J. Chem. Soc., Faraday Trans.* **1992**, *88*, 553. (b) Bandyopadhyay, B. N.; Harriman, A. *J. Chem. Soc., Faraday Trans. 1* **1977**, *73*, 663.
(58) (a) Luong, J. C.; Faltynek, R. A.; Wrighton, M. S. *J. Am. Chem. Soc.* **1980**, *102*, 7892. (b) Pomestchenko, I. E.; Polyansky, D. E.; Castellano, F. N. *Inorg. Chem.* **2005**, *44*, 3412.
(59) Tabata, H.; Fujii, M.; Hayashi, S.; Doi, T.; Wakabayashi, T. *Carbon* **2006**, *44*, 3168.
(60) Wada, Y.; Morisawa, Y.; Wakabayashi, T. *Chem. Phys. Lett.* **2012**, *541*, 54.
(61) (a) Wagner, J. R.; Hendricker, D. G. *J. Inorg. Nucl. Chem.* **1975**, *37*, 1375. (b) Gamelin, D. R.; George, M. W.; Glyn, P.; Grevels, F.-W.; Johnson, F. P. A.; Klotzbücher, W.; Morrison, S. L.; Russell, G.; Schaffner, K.; Turner, J. J. *Inorg. Chem.* **1994**, *33*, 3246.
(62) (a) Asbury, J. B.; Wang, Y.; Lian, T. *Bull. Chem. Soc. Jpn.* **2002**, *75*, 979. (b) Chudoba, C.; Nibbering, E. T. J.; Elsaesser, T. *Phys. Rev. Lett.* **1998**, *81*, 3010.
(63) (a) Okuyama, K.; Hasegawa, T.; Ito, M.; Mikami, N. *J. Phys. Chem.* **1984**, *88*, 1711. (b) Gutmann, M.; Gudipati, M.; Schönzart, P.-F.; Hohlneicher, G. *J. Phys. Chem.* **1992**, *96*, 2433.
(64) Moore, A. L.; Joy, A.; Tom, R.; Gust, D.; Moore, T. A.; Bensasson, R. V.; Land, E. J. *Science* **1982**, *216*, 982.
(65) (a) Wrighton, M. S.; Morse, D. L. *J. Am. Chem. Soc.* **1974**, *96*, 998. (b) Fredericks, S. M.; Luong, J. C.; Wrighton, M. S. *J. Am. Chem. Soc.* **1979**, *101*, 7415. (c) Wallace, L.; Jackman, D. C.; Rillema, D. P.; Merkert, J. W. *Inorg. Chem.* **1995**, *34*, 5210. (d) Striplin, D. R.; Crosby, G. A. *Coord. Chem. Rev.* **2001**, *211*, 163.
(66) (a) Nahhas, A. E.; Consani, C.; Blanco-Rodríguez, A. M.; Lancaster, K. M.; Braem, O.; Cannizzo, A.; Towrie, M.; Clark, I. P.; Záliš, S.; Chergui, M.; Vlček, A., Jr. *Inorg. Chem.* **2011**, *50*, 2932. (b) Blanco-Rodríguez, A. M.; Towrie, M.; Collin, J.-P.; Záliš, S.; Vlček, A., Jr. *Dalton Trans.* **2009**, 3941. (c) Blanco-Rodríguez, A. M.;

Ronayne, K. L.; Záliš, S.; Sykora, J.; Hof, M.; Vlček, A., Jr. *J. Phys. Chem. A* **2008**, *112*, 3506. (d) Dattelbaum, D. M.; Omberg, K. M.; Hay, P. J.; Gebhart, N. L.; Martin, R. L.; Schoonover, J. R.; Meyer, T. J. *J. Phys. Chem. A* **2004**, *108*, 3527. (e) Bredenbeck, J.; Helbing, J.; Hamm, P. *J. Am. Chem. Soc.* **2004**, *126*, 990.

(67) (a) Vlček, A., Jr.; Záliš, S. *Coord. Chem. Rev.* **2007**, *251*, 258. (b) Dattelbaum, D. M.; Omberg, K. M.; Schoonover, J. R.; Martin, R. L.; Meyer, T. J. *Inorg. Chem.* **2002**, *41*, 6071. (c) Blanco-Rodríguez, A. M.; Busby, M.; Ronayne, K.; Towrie, M.; Grădinaru, C.; Sudhamsu, J.; Sýkora, J.; Hof, M.; Záliš, S.; Di Bilio, A. J.; Crane, B. R.; Gray, H. B.; Vlček, A., Jr. *J. Am. Chem. Soc.* **2009**, *131*, 11788.

(68) (a) Liard, D. J.; Busby, M.; Matousek, P.; Towrie, M.; Vlček, A., Jr. *J. Phys. Chem. A* **2004**, *108*, 2363. (b) Cannizzo, A.; Blanco-Rodríguez, A. M.; Nahhas, A. E.; Šebera, J.; Záliš, S.; Vlćek, A., Jr.; Chergui, M. *J. Am. Chem. Soc.* **2008**, *130*, 8967.

(69) Holten, D.; Bocian, D. F.; Lindsey, J. S. *Acc. Chem. Res.* **2002**, *35*, 57.

(70) (a) Griffiths, M.; Sistrom, W. R.; Cohen-Bazire, G.; Stanier, R. Y. *Nature* **1955**, *176*, 1211. (b) Beddard, G. S.; Davidson, R. S.; Trethewey, K. R. *Nature* **1977**, *267*, 373.